



Synthesis and Characterization of Mango Wood Nanocellulose Fibers

J. K. Prasannakumar ^{a*‡}, G. K. Prakash ^b, B. E. Basavarajappa ^a and B. Suresh ^c

^a Department of Chemistry, Bapuji Institute of Engineering and Technology (Affiliated to Visvesvaraya Technological University, Belagavi) Davangere, Karnataka 577004, India.

^b Department of Chemistry, STJPU College, Davangere, Karnataka 577006, India.

^c Department of Civil Engineering, Bapuji Institute of Engineering and Technology (Affiliated to Visvesvaraya Technological University, Belagavi), Davangere, Karnataka 577004, India.

Authors' contributions

This work was carried out in collaboration among all authors. All authors read and approved the final manuscript.

Article Information

DOI: 10.9734/AJOCS/2022/v12i219145

Open Peer Review History:

This journal follows the Advanced Open Peer Review policy. Identity of the Reviewers, Editor(s) and additional Reviewers, peer review comments, different versions of the manuscript, comments of the editors, etc are available here: <https://www.sdiarticle5.com/review-history/90228>

Original Research Article

Received 05 June 2022
Accepted 09 August 2022
Published 11 August 2022

ABSTRACT

Agricultural biomasses are the prominent natural sources of cellulose currently available on the planet. When this was treated chemically, this acquire the properties such as toughness, good biocompatibility, and higher thermal stability. In this study, Nanocellulose was extracted from Mango wood (*Mangifera indica*) a largely available agricultural biomass. The cellulose was alkali-treated followed by bleaching to remove lignin and hemicellulose, pectins, and waxes. The green solvent i.e Ionic liquid (1-butyl-3-methylimidazolium chloride ([Bmim] Cl) was used to dissolve cellulose to yield Nanocellulose through sonication and centrifugation. The functional groups and significant conversion of cellulose to nanocellulose are confirmed by FT-IR spectra. The crystallinity of synthesized nanocellulose is illustrated by XRD. The surface architecture and size obtained are represented by SEM and TEM monographs. The TEM images show the synthesized nanocellulose has a dimension between 27.33 to 34.85 nm. The thermal stability of the obtained nanocellulose was evidenced using TGA/DTA. The thermal studies records that synthesized nanocellulose shows superior thermal stability up to 473.8°C. The efficient conversion of agricultural waste into value added material is achieved through a greener pathway.

Keywords: Mango wood; ionic liquid; lignin; cellulose; nanocellulose.

[‡] Research Centre;

*Corresponding author: E-mail: prassvin@gmail.com, prassvin@bietdvg.edu;

1. INTRODUCTION

As a result of population increase and industrial globalization, energy sectors around the world are encountering difficulties in meeting the energy demand and supply imbalance. Biomass, a carbon-neutral renewable resource obtained from the carbon-containing waste of various natural and anthropogenic processes, has emerged as the third key energy source to fill the energy gap, following coal and oil. Biomass could be generated from a variety of sources, including the timber industry besides, agriculture sector crops, forest raw materials, significant parts of domestic wastes, and wood. As a result, researchers and developers are increasing their focus aside from coal and oil and toward biomass, which will produce carbon-neutral energy and solve a range of problems such as management of solid waste, health implications, and bushfires [1].

As a developing nation, India has battled for decades to comply with global environmental and solid-waste management norms, which has been a significant obstacle. It generates an annual average of 960-1000 million tonnes of solid waste, with the agricultural sector accounting for a large portion of this [2]. Post-harvesting is responsible for about 13% of all solid waste made in Asia [3]. India is one of the top three countries that grow maize, paddy, and wheat, so researchers are most interested in how to use the type of cellulose that comes from these crops. The most under-utilized forms of cellulose, according to the current research scenario, are Rice husk, Sugarcane, Maize husk, and corn cob [4-5]. With 50% of the workforce employed in agriculture. India is self-sufficient in natural cellulose, and there is an abundance of bio-waste. Countries such as the United States, Europe, Canada, and Australia prioritize nanocellulose production due to its usage as commercial products [6-8]. In terms of nature, size, and function, nanocellulose is largely dependent on its parent cellulose.

Recent years have seen the growth of nanotechnology, which is interconnected with numerous other scientific disciplines and has an impact on all kinds of life [9]. Nanotechnology is a discipline of science that focuses on the development, modification, and application of materials with nanometer-scale dimensions. Nanotechnology is essential to the study of nanoparticles due to their diverse uses. [10]. Cellulose and lignocellulose nanoparticles play a

vital role in nanotechnology. Cellulosic materials are the most prevalent biological raw materials and can self-assemble into well-defined designs of numerous sizes, from nano to micro. Moreover, cellulose is a multipurpose raw material that can replace several non-renewable substances [11].

Cellulose nanocrystals (CNCs) and cellulose nanofibrils are the two major types of cellulose nanomaterials (CNs) that can be derived from a variety of plant and animal sources. Depending on their size and extraction process, cellulose nanocrystals may be referred to as cellulose nanowhiskers (CNW) or Nanocrystalline Cellulose (NCC) [12,13], and cellulose nanofibrils may be referred to as nanofibrillated cellulose (NFC) or Micro fibrillated Cellulose (MFC) [14]. Mango wood is derived from the mango tree. This is the same tree that produces the sweet fleshy fruit known as 'a mango', characterized by skin that turns from green to yellow/red and an inside comprised of a large stone surrounded by juicy yellow flesh. It's in the name *Mangifera indica*. The tree belongs to the Anacardiaceae family, which also includes Pistachio and Cashe.

The mango tree is evergreen and grows to an average height of between 15 and 18 meters (50 ft and 60 ft) [15].

Although mango trees are now widespread, they are indigenous to India, Myanmar (formerly Burma), and East Asia. Due to the popularity of its fruit, the tree is cultivated in many tropical climes. The wood is primarily grown in India, but the industry exists in many other countries, including Kenya and China. The natural colour of mango wood is light to a golden brown. However, mango wood is often beautiful discoloured due to 'spalting' referring to the different colours wood can turn in as a result of a fungus. Mango wood also shows prominent grain patterns, similar to oak and mahogany. These are highly sought after when polished. Mango wood is preferred for this study because this wood is comprised of about 25% lignin, and 70% cellulosic carbohydrates, with roughly 45% cellulose and 25% hemicelluloses [16]. The crystalline and amorphous areas of the fibrils are present in this cellulose. Acid hydrolysis of these regions can reduce the crystalline region's reactivity. This results in obtaining microfibrils, nanofibrils, and cellulose nanocrystals [17]. Because of their various biological origins, cellulose fibers have an intrinsic structural hierarchy. In recent years, the scientific and industrial communities have

become interested in the process of producing cellulose from various lignocellulosic fibers [18,19]. Because of the components that make up the native fibers, they are longitudinal, inflexible, and difficult to change.

The low lignin content in Mango Wood made it more appropriate for nanocellulose synthesis. Two common processes have been developed one is acid hydrolysis of nanocellulose, and the other is oxidation method, which uses TEMPO (2,2,6,6-tetramethylpiperidine-1-oxyl). Due to its diverse features, availability, and flexibility in reuse, the ionic liquid (IL) approach has been replacing these conventional methods in recent years. Naturally occurring cellulose is insoluble in the majority of solvents, however, it is soluble in IL.

Ionic liquids are a type of salt composed of cations and anions that are liquid at ambient temperature and are referred to as "green solvents." The increased use of these compounds in the pretreatment of lignocellulosic biomass is due to their unique physicochemical characteristics, which include adequate thermal and chemical stability, a low vapour pressure, and a high biopolymer-solvating capacity. Common ionic liquids for dissolving cellulose include 1-butyl-3-methylimidazolium chloride

(BmimCl), 1-allyl-3-methylimidazolium chloride (AmimCl), and 1-ethyl-3-methylimidazole acetate [20]. Recent research has identified ionic liquids as suitable solvents, swelling agents, and catalysts for nanocellulose synthesis. The major benefit of employing IL as a pretreatment is the reproducibility of insolvent recovery with minimum loss. It has been established that more than ninety percent of BmimCl's activity can be recovered by reusing it four times without losing its potency [21]. The use of IL as a nanocellulose surface modification medium has applications in nanomedicine and drug delivery, according to other researchers [22]. IL has recently been recommended as a reaction media for the homogenous production of cellulose. Therefore, according to some researchers, homogeneous cellulose acetylation can be accomplished in AmimCl without the need for catalysts, resulting in cellulose acetates with a wide range of substitution degrees [23]. The researchers have established the various properties of nanocellulose and preparation methods that yield cellulose in the nanoscale with nanofibers, nanocrystals, and nanofibrils and their thermal studies reveal that they show variable behavior based on the preparation methods adopted [24]. The purpose of this research is to transform agriculture biomass into value-added material through green synthesis and hence the

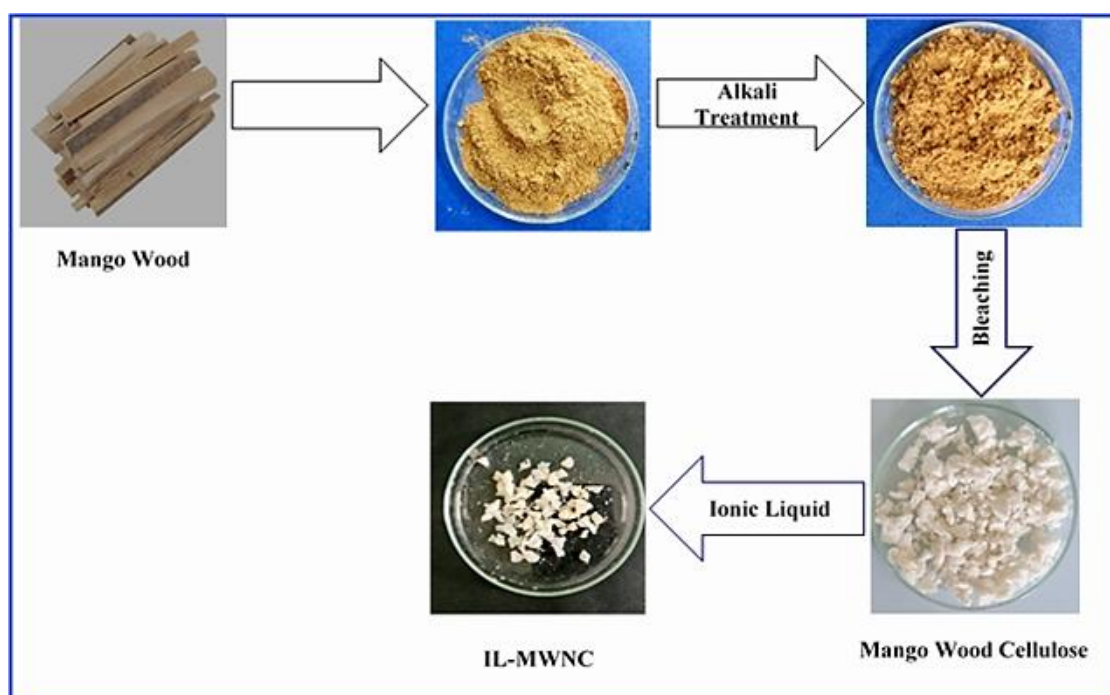


Fig. 1. Scheme of IL assisted synthesis of Nanocellulose

nanocellulose synthesized from Mango wood as illustrated in Fig. 1. FT-IR, X-Ray Diffraction, SEM, TEM, and Thermo Gravimetry studies were used to examine the functionality, crystallinity, and morphology, of synthesized nanocellulose. IL does not contribute to acid waste and is a more environmentally friendly method of isolating nanocellulose compared to conventional studies [25].

2. MATERIALS AND METHODS

The Lignocellulosic material such as Mango wood was collected from farmlands in and around Davanagere, Karnataka, India. The chemicals such as Chlorobutane (C₄H₉Cl) and 1-methylimidazole (CH₃C₃H₃N₂) were bought from Sigma Aldrich. NaClO₂, NaOH, and CH₃COOH were purchased from Merck and Qualigens Chemicals. All chemicals are used with a purity of 98 to 99% without purification.

2.1 Alkali Treatment

10 g of finely ground, sieved Mango Wood Powder treated with a 5% NaOH solution for 2 hours at temperatures ranging from 85°-100° C to remove hemicellulose. The obtained mass was filtered by repeated rinsing with distilled water until it reached a pH of 7. After that, the product is oven-dried for a day or until it reaches a constant weight. This process makes fiber more susceptible to bleaching, acid hydrolysis, and chemical modification.

2.2 Synthesis of Mango Wood Cellulose

After being treated with alkali, the sample is bleached to remove any remaining lignin. Alkali-treated samples were treated with a sodium chlorite solution containing approximately 5% sodium chlorite. The mixture was refluxed using a thermomagnetic stirrer between 90°-100° C for 3-4 hours by drop-wise addition of acetic acid to maintain acidic pH. Repetitive washing with distilled water eliminates residual lignin. The synthesized cellulose was filtered by deionized water washing until it reached a neutral pH. The obtained mass was oven-dried for one day or till it yields constant weight and stored for further process.

2.3 Synthesis of Ionic Liquid- (1-butyl-3-methyl-imidazolium chloride)

60 ml of 1-methyl imidazole (0.61 mol) and 80 ml of chlorobutane (0.76 mol) were taken in a two-necked round-bottomed flask immersed in an oil

bath to ascertain constant temperature. The mixture was kept for overnight refluxing at about 90°C-115°C with a magnetic stirrer until it gives yellow coloured transparent phase. After cooling the reaction mixture, the pure product in the form of an oil or solid was obtained.

2.4 Nanocellulose Synthesis in 1-butyl-3-methylimidazolium Chloride Ionic Liquid Solvent

Mango wood Nanocellulose (IL-MWNC) was synthesized by adding 10g of 1-butyl-3-methylimidazolium chloride ionic liquid into a 100 ml dry two-necked flask fitted with a water-cooled condenser and carries calcium guard tube at the outlet of the condenser. It was then placed in an oil bath. 1g of finely ground and dried Mango Wood Cellulose was added slowly into a flask containing the above ionic liquid and refluxed on a thermomagnetic stirrer at 115°-120°C for 1.5 hr. By dissolving cellulose in ionic liquid, a pale yellow solution is obtained. The mixture was then appeared by adding 50 ml of ice-cold distilled water. The resulting nanocellulose precipitate was filtered, washed 5-6 times with cold distillate water, dried, and stored. It is used in the name IL-MWNC.

2.5 Cellulose Dissolution Mechanism in Ionic Liquid

In order to directly synthesize cellulose solutions, Graenacher has filed a patent on the use of molten quaternary ammonium salts in the manufacture of cellulose and ionic liquids have been used in this process [26]. According to the theory put forth by Swatloski et al., cellulose can be directly dissolved by ionic liquids (combinations of halide anions and imidazolium cations) with just moderate heating or microwaving [27,28]. Furthermore, some research groups have demonstrated that a mixture of ionic liquid combinations and conditions can dissolve cellulose [29]. Fig. 2 depicts the cellulose dissolution mechanism. The anion of the ionic liquid interacts favorably via hydrogen bonding with the hydroxyl protons of cellulose, thereby breaking the strong intermolecular hydrogen bonds that exist between carbohydrate chains and promoting dissolution [30].

2.6 Characterizations

The FTIR of Cellulose, IL-MWNC was recorded with Thermo Nicolet iS50. After being mixed with KBr powder, the samples were pressed into thin

pellets. The sample's wavelength range was measured to be between 4000 and 400 cm^{-1} . The XRD data were recorded using a Bruker D8 Advance Diffractometer. The crystalline and amorphous zone peak heights were measured, and the crystallinity index (CI) was calculated using Scherer's formula with a 0.02 step size. The Jeol 6390LA/ OXFORD XMX N instrument used to capture SEM (Scanning Electron Microscopy) images had an acceleration voltage range of 0.5 to 30 kV. A secondary electron (SE) detector was used to acquire the images. TEM images were recorded using a 200 kV, LaB6 electron gun with a 0.23 nm point resolution and 0.14 nm lattice resolution. TGA (Thermogravimetric Analysis) and DTA were performed using the Perkin Elmer STA 6000 instrument (Differential Thermal Analysis).

3. RESULTS AND DISCUSSION

3.1 FTIR Analysis

The chemical functional groups of cellulose were investigated using FTIR. FTIR of IL-MWNC is shown in Fig. 3. Both have similar cellulose-I structured absorption peaks between 3328.51 and 3331.89 cm^{-1} , owing to -OH stretching vibrations caused by hydrogen bonding. The peaks at 2892.52 to 2893.39 cm^{-1} ascribe C-H stretching vibrations. Whereas, the peaks between 1636.06 and 1641.23 cm^{-1} are caused by the H-O-H deformation of absorbed water and conjugated C=O stretch vibrations. The region of absorption between 1428.27 cm^{-1} was attributed to asymmetric C-H deformation, which shifted to a low wavenumber and became weaker due to a

reaction at higher temperatures with IL. The breaking of H-bonding at O-6. C-O antisymmetric bridge stretching is represented by the peak at 1161.34 cm^{-1} . The C-O-C pyranose ring skeletal vibration was assigned peaks ranging from 1029.99 to 1061.60 cm^{-1} . In cellulose, the peaks at 897.09 cm^{-1} correlate to glycosidic linkage whereas it disappeared in IL-MWNC indicating efficient transformation. Absorption peaks moving to higher wavenumbers showed the transition from cellulose I to cellulose II. The result shows that there was no other intervening reaction in the middle of the dissolving process.

3.2 XRD Analysis

XRD analysis shows that nanocellulose can be found to be crystalline. Fig. 4 shows the X-ray diffraction pattern of IL-MWNC which was ionic liquid treated. These XRD patterns depict semicrystalline materials with an amorphous wide hump and crystalline peaks. IL-MWNC exhibits its 2θ values in the range between 15.50°, 22.783°, and 35.0° attributed to low crystallinity, whereas cellulose shows the peak at 15.50°, 22.50° and 35.0. This represents the cellulose-I structure, furthermore, the sonication and centrifugation do not affect the principal cellulose structure besides cavitation also does not affect the cellulose structure. Due to the disruption of intermolecular and intramolecular hydrogen bonds of cellulose by the ionic liquid, the crystallinity index of the synthesized nanocellulose is reported to be slightly decreased than that of cellulose.

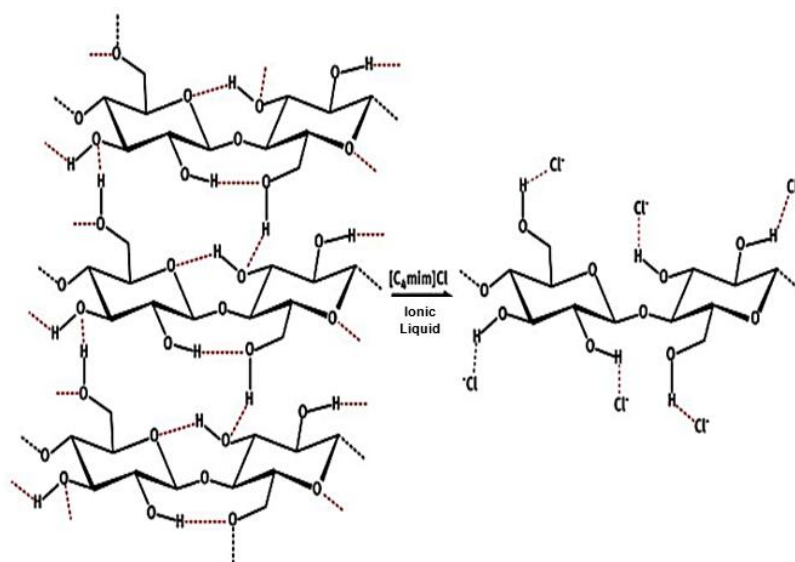


Fig. 2. Dissolution of cellulose with ionic liquid

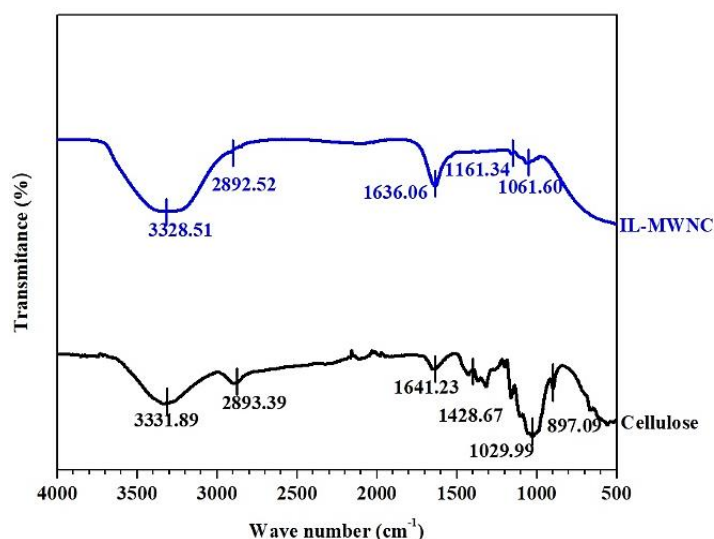


Fig. 3. FTIR of Cellulose, IL-MWNC

3.3 SEM Analysis

High-resolution surface imaging is possible using a scanning electron microscope. Using an electron beam, the SEM produces images of the surface. Prepared nanocellulose was found to be fibrous with considerable aggregation, as seen by SEM images. The surface morphology is depicted in the SEM images. This shows nanoscale dimensions, including uneven cross-sections, and a vast number of microscopic microfibrils, as well as various forms, and non-uniform surfaces and are correlated with cellulose [31-32]. Fig. 5 shows the morphology of IL-MWNC corresponds to nanosized fibers which are regularly structured ones. Here,

individualized nanofibers can be obtained with ultrasonic treatment.

3.4 TEM Analysis

The TEM images of IL-MWNC were obtained to analyze the internal morphology & structure of the synthesized nano cellulose, as shown in Fig. 6. The TEM image indicates that the nanocellulose obtained is in the form of nanofibers. Nanofibers are cage-like distinct and readily visible. Even the tendency to agglomerate can be seen in all of the images. The IL-MWNC reveals nanofibers of the length of several microns and with an average diameter between 27.33 and 34.85 nm that are regularly organized and correlated with cellulose fibers [33,34].

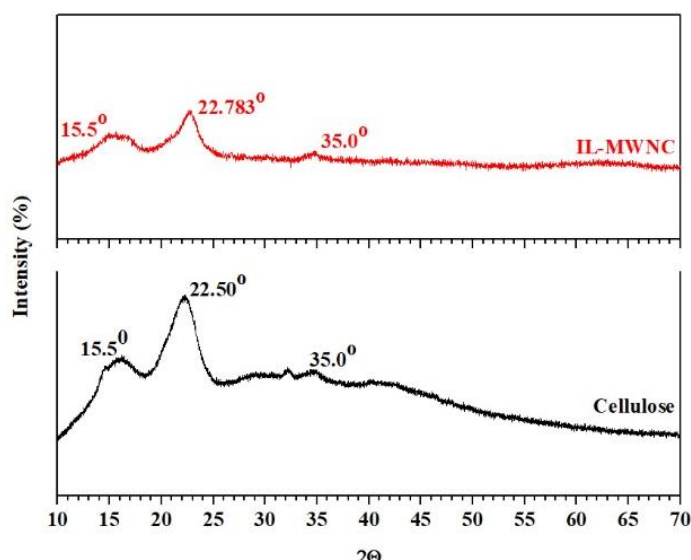


Fig. 4. XRD pattern of IL-MWNC, and cellulose

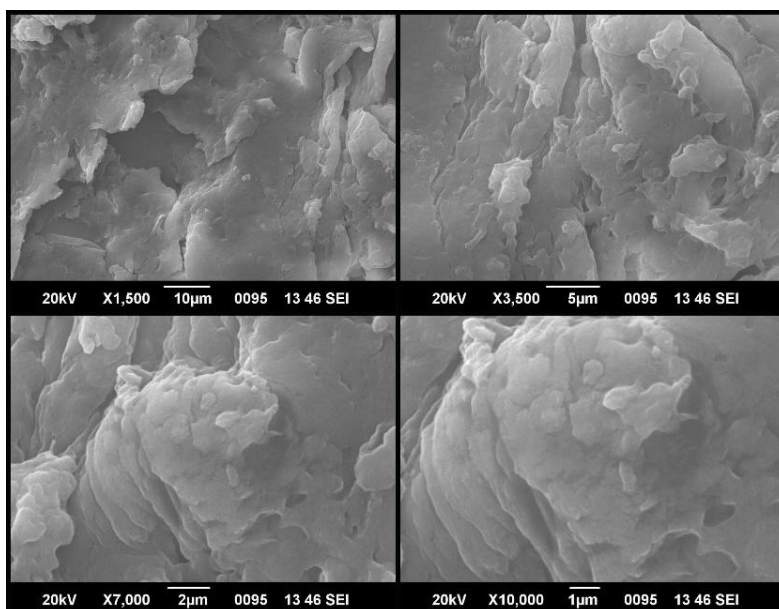


Fig. 5. SEM monographs of IL-MWNC

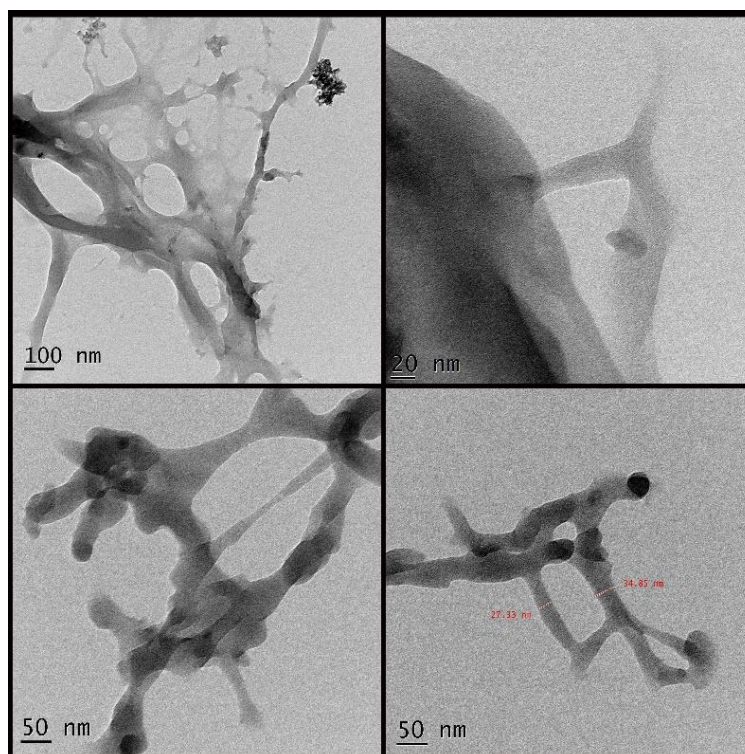


Fig. 6. TEM image of IL-MWNC

This is inferred from the above observation that the synthesized nanocellulose well exhibits nanoscale dimensions. Structured nanofibers can be seen in IL-MWNC. The above analysis reveals that the ionic liquid readily dissolves the cellulose which affects the morphology and size distribution of synthesized nanocellulose.

3.5 TGA/DTA Analysis

The thermal stability of the IL-MWNC was examined in comparison with the standard Nanocellulose sample by using TGA, and the DTA curves are shown in Fig. 7 and Fig. 8 respectively. The water evaporation in the

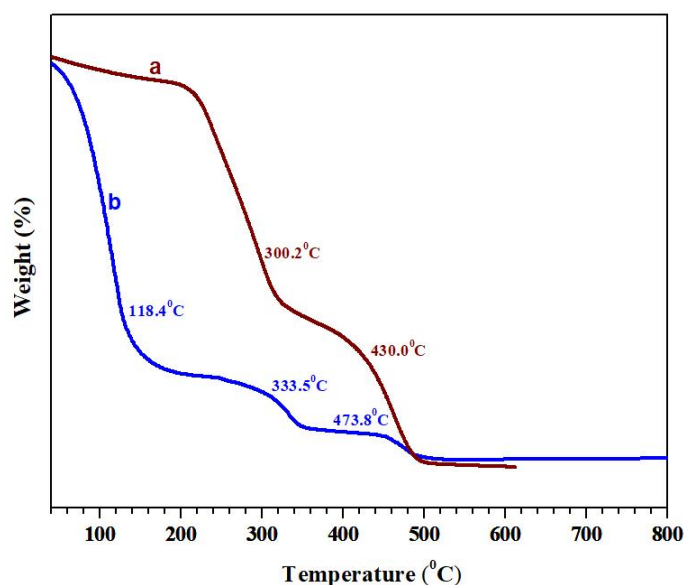


Fig. 7. TGA of a) Nanocellulose b) IL-MWNC

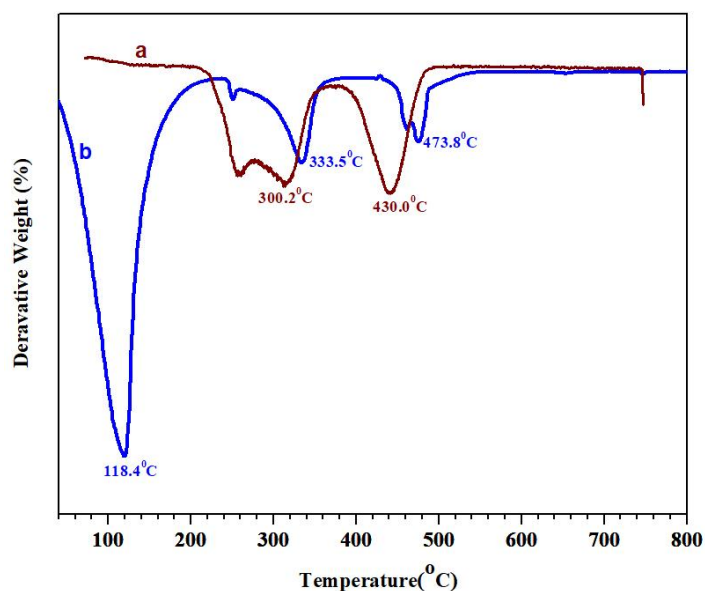


Fig. 8. DTG of a) Nanocellulose b) IL-MWNC

synthesized nanocellulose is observed between 80°C to 120.0°C. The degradation temperature of IL-MWNC is 250.1°C, 458.4°C, and 473.8°C. Whereas the Nanocellulose samples ascribe degradation temperature of 300.2°C and 430°C. The major weight loss between 250.0°C and 333.5°C regions indicates the depolymerization of hemicellulose and glycosidic linkages and they have broken. The onset degradation temperature is found to be 260°C. Here the weight loss occurred in three stages, the first stage was associated with evaporation of water the second and third stage of weight loss occurred in the

range of 333.5°C to 473.8°C. The weight loss occurred in Nanocellulose in two stages 300°C and 430°C. The results depict that the significance of synthesized nanocellulose in ionic liquid shows superior thermal stability of 473.8°C when compared to Nanocellulose and Cellulose in general [35,36].

4. CONCLUSION

In the present study, Mango wood is an abundantly available lignocellulosic agricultural biomass utilized to produce nanocellulose from

an ionic liquid. The FTIR spectra suggest that IL-MWNC exhibits the same distinctive cellulose peaks. The finding reveals that there was no derivational reaction during the cellulose dissolution process. According to X-ray crystallographic investigations, synthesized nanocellulose is semicrystalline in nature with an amorphous wide hump and crystalline peaks. It implies that the hydrogen bonds of cellulose were disrupted, resulting in the disintegration of the crystal structure during the entire process. Different shapes with a non-uniform surface, regular cross-sections, and a great number of microscopic microfibrils can be seen in SEM images. TEM images show that the cellulose synthesized is in the nanoscale dimension. The cellulose is apparently dissolved by the ionic liquid, a promising green solvent, which impacts the morphology and size distribution of produced cellulose in nanometre size. According to TGA/DTA analysis, samples exhibit a minor weight loss of roughly 80°C-120°C, which is attributed to the evaporation of water bound in the cellulose samples. The strong troughs in the DTA curve reveal that the onset of the breakdown of ionic liquid treated cellulose is 333°C. IL-MWNC has shown higher thermal stability. TGA revealed that IL-MWNC treated with ionic liquid has a higher degradation temperature (473.8°C), indicating greater thermal stability. As a result of high thermal resistance, this can be used in the manufacture of high-temperature resistant materials. Due to their smaller size, these can be used to manufacture high strength nanocomposites. The fibrous nanocellulose can be used for photocatalytic dye degradation and for the removal of heavy metals from the effluent. Furthermore, this research seeks to demonstrate the remarkable practical application of synthesized nanocellulose from agricultural biomass, which will undoubtedly meet India's need for solid waste management and reduce chemical waste through a more realistic approach to nanocellulose manufacturing.

ACKNOWLEDGEMENTS

The authors are grateful to the management, Director, and Principal of Bapuji Institute of Engineering and Technology, Davanagere, Karnataka for providing all the facilities to perform this research. The authors remain thankful to the Sophisticated Test and Instrumentation Centre (STIC), Cochin, Kerala for having provided the analysis data.

COMPETING INTERESTS

Authors have declared that no competing interests exist.

REFERENCES

1. Sharma A. and Mohanty B. Thermal degradation of mango (*Mangifera indica*) wood sawdust in a nitrogen environment: Characterization, kinetics, reaction mechanism, and thermodynamic analysis. RSC Advances. 2021;11(22):13396-13408. Available: <https://doi.org/10.1039/d1ra01467f>
2. Katare VD, Madurwar MV. Experimental characterization of sugarcane biomass ash—A review. Construction and Building Materials. 2017;152:1-15. Available: <https://doi.org/10.1016/j.conbuildmat.2017.06.142>
3. Youshizawa S, Tanaka M and Shekder A V. Global Trends in Waste Generation in Recycling, Waste Treatment, and Clean Technology, TMS Mineral, Metals and Materials Publishers. Spain. 2001;1541-1552.
4. Jagadesh P, Ramachandramurthy A, Murugesan R. Evaluation of mechanical properties of Sugar Cane Bagasse Ash concrete. Construction and Building Materials. 2018;176:608-617. Available: <https://doi.org/10.1016/j.conbuildmat.2018.05.037>
5. Reddy N. and Yang Y. Properties and potential applications of natural cellulose fibers from cornhusks. Green Chemistry. 2005;7(4):190-195. Available: <https://doi.org/10.1039/B415102J>
6. Lin N, Dufresne A. Nanocellulose in biomedicine: Current status and future prospect. European Polymer Journal. 2014;59:302-325. Available: <https://doi.org/10.1016/j.eurpolymj.2014.07.025>
7. Das S, Ghosh Bm Sarkar K. Nanocellulose as sustainable biomaterials for drug delivery. Sensors International. 2022;3: 100135. Available: <https://doi.org/10.1016/j.sintl.2021.100135>
8. Klemm D, Kramer F, Moritz S, Lindström T, Ankerfors M, Gray D, Dorris A., Nanocelluloses: A new family of nature-based materials. Angewandte Chemie International Edition. 2011;50(24): 5438-5466.

- Available:<https://doi.org/10.1002/anie.201001273>
9. Baker S, Satish S. Endophytes: Toward a vision in synthesis of nanoparticle for future therapeutic agents. *Int. J. Bio-Inorg. Hybd. Nanomat.* 2012; 1(2):67-77.
 10. Kavitha KS, Baker S, Rakshith D, Kavitha HU, Yashwantha Rao HC, Harini BP, Satish S. Plants as green source towards synthesis of nanoparticles. *Int Res J Biol Sci.* 2013;2(6):66-76.
 11. Wegner TH, Jones PE. Advancing cellulose-based nanotechnology. *Cellulose.* 2006;13(2):115-118. Available:<https://doi.org/10.1007/s10570-006-9056-1>
 12. Fortunati E, Puglia D, Monti M, Peponi L, Santulli C, Kenny JM, Torre L. Extraction of cellulose nanocrystals from *Phormium tenax* fibres. *Journal of Polymers and the Environment.* 2013;21(2):319-328. Available:<https://doi.org/10.1007/s10924-012-0543-1>
 13. Dong H, Snyder JF, Tran DT, Leadore JL. Hydrogel, aerogel and film of cellulose nanofibrils functionalized with silver nanoparticles. *Carbohydrate Polymers.* 2013;95(2):760-767. Available:<https://doi.org/10.1016/j.carbpol.2013.03.041>
 14. Bledzki AK, Gassan J. Composites reinforced with cellulose based fibres. *Progress in polymer science.* 1999;24(2): 221-274. Available:[https://doi.org/10.1016/S0079-6700\(98\)00018-5](https://doi.org/10.1016/S0079-6700(98)00018-5)
 15. loelovich M. Optimal conditions for isolation of nanocrystalline cellulose particles. *Nanoscience and Nanotechnology.* 2012;2(2):9-13. DOI: 10.5923/j.nn.20120202.03
 16. loelovich Michel, Leykin Alex, Haemek M. Formation nano-structure of microcrystalline cellulose. *Cell. Chem. Technol.* 2006;40(5):313-317.
 17. Potthast A, Röhring J, Rosenau T, Borgards A, Sixta H, Kosma P. A novel method for the determination of carbonyl groups in cellulose by fluorescence labeling. 3. Monitoring oxidative processes. *Biomacromolecules.* 2003;4(3):743-749.
 18. Barrer, R. M. The viscosity of pure liquids. II. Polymerised ionic melts. *Transactions of the Faraday Society.* 1943; 39:59-67. Available:<https://doi.org/10.1039/TF943390059>
 19. Pinkert A, Marsh KN, Pang S, Staiger MP. Ionic liquids and their interaction with cellulose. *Chemical reviews.* 2009;109(12): 6712-6728. Available:<https://doi.org/10.1021/cr9001947>
 20. Babicka M, Woźniak M, Szentner K, Bartkowiak M, Peplińska B, Dwiecki K, et al. Nanocellulose production using ionic liquids with enzymatic pretreatment. *Materials.* 2021; 14(12):3264. Available:<https://doi.org/10.3390/ma14123264>
 21. Phanthong P, Karnjanakom S, Reubroycharoen P, Hao X, Abudula A, Guan G. A facile one-step way for extraction of nanocellulose with high yield by ball milling with ionic liquid. *Cellulose.* 2017;24(5):2083-2093. Available:<https://doi.org/10.1007/s10570-017-1238-5>
 22. Haron GAS, Mahmood H, Noh MH, Alam MZ, Moniruzzaman M. Ionic liquids as a sustainable platform for nanocellulose processing from bioresources: Overview and current status. *ACS Sustainable Chemistry & Engineering.* 2021;9(3):1008-1034. Available:<https://doi.org/10.1021/acssuschemeng.0c06409>
 23. Turner MB, Spear SK, Holbrey JD, Rogers RD. Production of bioactive cellulose films reconstituted from ionic liquids. *Biomacromolecules.* 2004;5(4):1379-1384. Available:<https://doi.org/10.1021/bm049748q>
 24. Shamsuri AA, Abdan K. Nanocellulose Extraction Using Ionic Liquids: Syntheses, Processes, and Properties. *Frontiers in Materials.* 2022;358.
 25. Pal N, Hoteit H. and Mandal A. Structural aspects, mechanisms and emerging prospects of Gemini surfactant-based alternative Enhanced Oil Recovery technology: A review. *Journal of Molecular Liquids.* 2021;339:116811. Available:<https://doi.org/10.1016/j.molliq.2021.116811>
 26. Graenacher C U.S. Patent ,1993 1:943,176.
 27. Swatloski RP, Spear SK, Holbrey JD, Rogers RD. *J. Am. Chem. Soc.* 2002;124:4974. Available:<https://doi.org/10.1039/B204469B>
 28. Swatloski RP, Holbrey JD, Rogers RD. U.S. Patent. 2002;6(824):599 B2.

29. Wang H, Gurau G, Rogers R D. Chem. Soc. Rev. 2012;41:1519–37
30. Remsing Richard C, Swatloski Richard P, Rogers Robin D and Moyna. Guillermo. Mechanism of cellulose dissolution in the ionic liquid 1-n-butyl-3-methylimidazolium chloride: A ¹³C and ^{35/37}Cl NMR relaxation study on model systems. Chemical Communications. 2006;12:1271–1273. Available:https://doi.org/10.1039/B600586C
31. Zhang LY, Tsuzuki T, Wang XG. Preparation and characterization on cellulose nanofiber film. In Materials science forum. Trans Tech Publications Ltd. 2010; 654:1760-1763.
32. Wattanakornsiri A, Pachana K, Kaewpirom S, Sawangwong P, Migliaresi C. Green composites of thermoplastic corn starch and recycled paper cellulose fibers. Songklanakarin Journal of Science and Technology. 2011; 33:461-467.
33. Kurei T, Hioki Y, Kose R, Nakaba S, Funada R & Horikawa Y. Effects of orientation and degree of polymerization on tensile properties in the cellulose sheets using hierarchical structure of wood. Cellulose. 2022;29:1-14. Available:https://doi.org/10.1007/s10570-021-04160-7.
34. Gao K, Shao Z, Li J, Wang X, Peng X, Wang W, Wang F. Cellulose nanofiber–graphene all solid-state flexible supercapacitors. J. Mater. Chem. 2012; A1(2012):63-67. Available:https://doi: 10.1039/c2ta00386d
35. Sharma A, Mandal T, Goswami S. Cellulose nanofibers from rice straw: Process development for improved delignification and better crystallinity index. Trends in Carbohydrate Research. 2018; 9(4).
36. Thakur M, Sharma A, Ahlawat V, Bhattacharya M, Goswami S. Process optimization for the production of cellulose nanocrystals from rice straw derived α -cellulose. Materials Science for Energy Technologies. 2020;3. Available:https://doi.org/10.1016/j.mset.2019.12.005

© 2022 Prasannakumar et al.; This is an Open Access article distributed under the terms of the Creative Commons Attribution License (<http://creativecommons.org/licenses/by/4.0>), which permits unrestricted use, distribution, and reproduction in any medium, provided the original work is properly cited.

Peer-review history:

The peer review history for this paper can be accessed here:
<https://www.sdiarticle5.com/review-history/90228>